Atmospheric effects on satellite gravity gradiometry data

Mehdi Eshagh, Lars E. Sjöberg

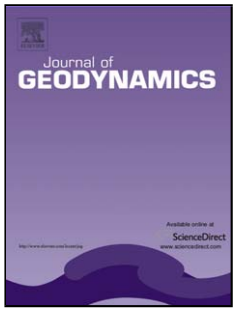

Title: Atmospheric effects on satellite gravity gradiometry data

Authors: Mehdi Eshagh, Lars E. Sjöberg

PII: S0264-3707(08)00044-6
DOI: doi:10.1016/j.jog.2008.06.001
Reference: GEOD 852

To appear in: *Journal of Geodynamics*

Received date: 25-1-2008
Revised date: 30-5-2008
Accepted date: 5-6-2008

Please cite this article as: Eshagh, M., Sjöberg, L.E., Atmospheric effects on satellite gravity gradiometry data, *Journal of Geodynamics* (2007), doi:10.1016/j.jog.2008.06.001

Atmospheric effects on satellite gravity gradiometry data

Mehdi Eshagh and Lars E. Sjöberg
Royal Institute of Technology, SE-10044, Stockholm, Sweden
Phone:+46 8 7907369; Fax: +46 8 7907343
Emails:eshagh@kth.se
sjoberg@kth.se

Abstract
Atmospheric masses play an important role in precise downward continuation and validation of satellite gravity gradiometry data. In this paper we present two alternative ways to formulate the atmospheric potential. Two density models for the atmosphere are proposed and used to formulate the external and internal atmospheric potentials in spherical harmonics. Based on the derived harmonic coefficients, the direct atmospheric effects on the satellite gravity gradiometry data are investigated and presented in the orbital frame over Fennoscandia. The formulas of the indirect atmospheric effects on gravity anomaly and geoid (downward continued quantities) are also derived using the proposed density models. The numerical results show that the atmospheric effect can only be significant for precise validation or inversion of the GOCE gradiometric data at the mE level.

Keywords: satellite gradiometry, direct and indirect atmospheric effects, atmospheric density

1. Introduction

Satellite gravity gradiometry (SGG) is a technique by which the second order derivatives of the gravitational potential are measured based on differential accelerometry. The atmospheric masses below satellites affect SGG data. The Gravity field and Ocean Circulation Explorer (GOCE) [see e.g. Balmino et al. (1998, 2001), ESA (1999), Albertella et al. (2002)] is an upcoming satellite mission based on this technique, and it is expected to produce an Earth's gravity field model with an improved resolution from space. The SGG data can directly be continued downward to the sea level for the local gravity field determination. Therefore it is necessary to consider the gravitational effects of the topography and static atmosphere to smooth the gravity field and simplify the downward continuation process. Temporal variations of the atmospheric density are beyond the scope of this paper, but such variations will be an obligatory part of data processing of GOCE as it was for GRACE as well [Flechtner et al. 2006]. These effects should also be considered if validation of the SGG data is of interest. The topographic effect has largely been investigated by many scientists and in different applications; see e.g., Martinec et al. (1993), Martinec and Vaníček (1994), Sjöberg (1998), Sjöberg and Nahavandchi (1999), Sjöberg (2000, 2007), Tsoulis (2001), Heck (2003), Seitz and Heck (2003), Wild and Heck (2004a, 2004b), Makhloof and Ilk (2005, 2006), Makhloof (2007) and Eshagh and Sjöberg (2008a, 2008b).

Some primary assumptions are needed for considering the atmospheric effects. The atmosphere is usually assumed to be layered spherically above a sphere approximating the Earth surface. Also Moritz (1980), Sjöberg (1993, 1998, 1999, 2001), Sjöberg and Nahavandchi (1999) and Nahavandchi (2004) used spherical approximation of sea level and considered the topographic heights with respect to this sphere. Similar assumptions are considered for the atmospheric density through this study although we know that the semi-major axis of the ellipsoidal Earth is 21 km longer than the semi-minor one, this approximation results an overestimation and an underestimation in the atmospheric effect at the poles and equator, respectively. In order to solve this problem the ellipsoidal harmonics should be used and more complicated formulation is needed which is not in scope of this paper neither. This matter was well investigated by Sjöberg (2006).

Ecker and Mittermayer (1969) used an ellipsoidal approach to study the atmospheric gravitational potential and acceleration; they proposed a mathematical model for the direct atmospheric effect (DAE), which is well-known as the IAG (International Association of Geodesy) approach. Anderson et al. (1975) considered the effect of the atmospheric masses in physical geodesy problems and computed the global values of the atmospheric effect on gravity and the geoid. Sjöberg (1993) investigated the effect of terrain in the atmospheric gravity and geoid corrections, Sjöberg (1998) presented the atmospheric correction on the gravity anomaly, geoid and on the satellite derived geopotential coefficients. Sjöberg (1999) found some shortcomings in the IAG approach in atmospheric geoid correction and proposed a new strategy to solve them. Sjöberg and Nahavandchi (2000) investigated the direct and indirect effect of the atmosphere in modified Stokes' formula and they showed that the DAE on the geoid can reach 40 cm. Novák (2000) presented a density model for the atmosphere based on a simple polynomial fitting and used that model to compute the atmospheric effect on the geoid. The polynomial function was used only for atmospheric mass density modeling within the topography, i.e., below the elevation of highest spot on the Earth (approximately 10 km above the mean sea level). The atmospheric masses above 10 km elevation can be considered by using United States Standard Atmospheric model (USSA76)[United State atmosphere, 1976]. For more details about his method see e.g. Novák (2000). Sjöberg (2001) investigated the atmospheric correction and found that the atmosphere contributes with the zero-degree harmonic of magnitude of 1 cm on the geoid. Nahavandchi (2004) presented another strategy for the direct atmospheric gravity effect in geoid determination. He numerically compared his new strategy with old formulas in Iran and found 17 cm difference on the geoid between both formulas in that region, but as Sjöberg (1998) argued the direct effect is considerably reduced after restoring the atmospheric effect. Sjöberg (2006) showed that the atmospheric effect in geoid determination needs a correction for the geometry when applying the spherical approximation of Stokes formula. According to his conclusions the correction needed to the atmospheric effect in spherical Stokes formula varies between 0.3 and 4.0 cm on the geoid at the equator and pole, respectively. Tenzer et al. (2006) considered the effect of atmospheric masses for Stokes problem with concentration on the direct and secondary indirect atmospheric effects. They found the complete effect of the atmosphere on the ground gravity anomaly varies between 1.75 and 1.81 mGal in Canada, and the effects are mainly dependent on the accuracy of the atmospheric density model (ADM). Novák and Grafarend (2006) proposed a method to compute the effect of topographic and atmospheric masses on spaceborne data based on spherical harmonic expansion with a numerical study in North America.

In this paper, another approach to the atmospheric effect on the SGG data is proposed than that used by Novák and Grafarend (2006). The main difference is related to the used ADM.

We expand the atmospheric potential in spherical harmonics based on the Kunglia Tekniska Högskolan Atmospheric density model (KTHA) and we modify that model based on the USSA76 and compare it with the original KTHA. Finally, we propose a new KTHA (NKTHA) based on Novák's atmospheric density model (NADM) and the KTHA. The DAE on the SGG are derived in orbital frames over Fennoscandia; and their statistics, based on different methods, are compared and discussed. Since the SGG can be continued downward using inversion of second order derivatives of the extended Stokes or Abel-Poisson integrals, we will formulate the internal type of the gravitational effect of the atmosphere on gravity anomaly and geoid (restoration of the atmospheric effects) as the results of the inversion. It should be mentioned that such gravitational effect, can be considered on the downward continued SGG data too. The paper is arranged as follows.

In the next section different ADMs including the NKTHA are introduced. In Sections 3 and 4 we formulate the external and internal atmospheric gravitational potentials in spherical harmonics based on the KTHA and NKTHA, respectively. In Section 5 we explain how to compute the DAE on the SGG data in the orbital frame. Section 6 presents the formulas for the indirect atmospheric effects (IAE) on the gravity anomaly and geoid. Section 7 deals with numerical studies on the ADMs and DAE on the SGG data over Fennoscandia, and the article is ended by the conclusions in Section 8.

2. Atmospheric density models (ADMs)

There are different models for the density of the atmosphere. One of the most well-known models was issued by NOAA (National Oceanic and Atmospheric Administration), NASA (National Aeronautics and Space Administration) and USAF(United State Air Force) as United States Standard Atmospheric model in 1976 (USSA76) [United State Standard Atmosphere, 1976]. This model is a complicated model depending on atmospheric pressure and molecular-scale temperature. For considering these parameters, the atmospheric masses (up to the height of 86 km), are divided into seven layers, and in each layer a molecular-scale temperature and pressure are defined according to some other mathematical models. However, this model is not preferred in geodesy, and simpler approximating models are sought. In the following we review two ADMs and present a new ADM which is formulated based on the two previous ADMs.

2. 1 KTH atmospheric density model (KTHA)

Sjöberg (1998) assumed that the atmospheric density is laterally layered and changes only with elevation. This assumption is not so far from reality as the atmospheric density reduces by increasing height. Based on the results of Ecker and Mittermayer (1969) which were derived from the US standard atmospheric density model presented in 1961 (USSA61) [Reference Atmosphere Committee, 1961], Sjöberg (1998) proposed the following ADM:

$$\rho^{a}\left(r\right)=\rho_{0}\left(\frac{R}{r}\right)^{\nu}, \tag{1}$$

where, $\rho^{a}\left(r\right)$ is the atmospheric density, R (set to 6378137 m) is the Earth's mean radius, $R \le r \le R+Z$ is the geocentric radius of any point inside the atmosphere, , ρ_{0} =1.2227 kg/ m^{3} is the atmospheric density at the sea level, and $\nu = 850$ is an estimated constant. We name this model KTHA.

2.2 Novák's atmospheric density model (NADM)

The maximum value of the atmospheric density is at the sea level and decreases fast with increasing elevation. Novák (2000) proposed the following model to approximate the vertical behaviour of the atmospheric density (NADM):

$$\rho^{a}(r)=\rho_{0}\left[1+\alpha H+\beta H^{2}\right], \tag{2}$$

where, $\alpha = -7.6495\times10^{-5}\ m^{-1}$, $\beta = 2.2781\times10^{-9}\ m^{-2}$ and H = r-R with $0 \le H < 10$ km. The other parameters of this model are the same as defined in previous section. As Novák (2000) mentioned his model fits the USSA76 with the accuracy of about 10^{-3} to up to 10 km above sea level. For higher elevations the USSA76 should be used.

2.3 New KTH atmospheric density model (NKTHA)

We now propose the following model (NKTHA) for the atmospheric density, which in fact is a direct combination of the NADM and KTHA:

$$\rho^{a}(r)=\begin{cases}\rho_{0}\left[1+\alpha H+\beta H^{2}\right], & 0\le H\le H_{0}\\ \rho^{a}(H_{0})\left(\dfrac{R+H_{0}}{r}\right)^{\nu''}, & H_{0}\le H\le Z\end{cases}, \tag{3}$$

where H_0 =10 km and $\rho^{a}(H_0)$=0.4127 kg/ m^3 is based on the NADM. By using this ADM we approximate the atmospheric density at higher levels by a simple mathematical model and it can be considered up to the satellite level. The parameter ν''=890 was derived based on a simple least-squares fit to the USSA76 elevations of above 10 km.

3. Atmospheric potential based on KTHA

In this section we derive the atmospheric potentials considering the KTHA as the ADM. The atmospheric potential can be expressed according to the well-known Newtonian volume integral as

$$V^{a}(P)=G\iint_{\sigma}\int_{r_S}^{r_Z}\rho^{a}(r_Q)\frac{r_Q^{2}dr_Q}{l_{PQ}}d\sigma, \tag{4}$$

where, G is the Newtonian gravitational constant, $V^{a}(P)$ stands for the atmospheric potential at point P, $\rho^{a}(r_Q)$ is the atmospheric density function at point Q (integration point), σ is the full solid angle of integration, r_S and r_Z are the topographic surface, and the upper limit of the atmosphere, l_{PQ} is the distance between computation point P and integration point Q. dr_Q and $d\sigma$ are the radial and horizontal integration elements, respectively. In order to obtain the external atmospheric potential $1/l_{PQ}$ is expanded into a Legendre series of external type as:

$$\frac{1}{l_{PQ}} = \frac{1}{r_P}\sum_{n=0}^{\infty}\left(\frac{r_Q}{r_P}\right)^n P_n\left(\cos\psi_{PQ}\right). \tag{5}$$

where $r_P \geq r_Q$ is the geocentric radius of the computation point P, and ψ_{PQ} is the geocentric angle between P and Q. By substituting Eq. (5) into Eq. (4) and considering Eq. (1) as the ADM we have:

$$V_{ext}^a(P) = G\sum_{n=0}^{\infty}\rho_0 \frac{R^{\nu}}{r_P^{n+1}}\iint_{\sigma}\int_{r_S}^{r_Z} r_Q^{n+2-\nu} dr_Q P_n\left(\cos\psi_{PQ}\right)d\sigma, \tag{6}$$

and after integrating radially and regarding $r_S = R + H$ and $r_Z = R + Z$ (where H is a function of position whereas Z is a constant) we obtain

$$V_{ext}^a(P) = G\rho_0\sum_{n=0}^{\infty}\frac{R^{n+3}}{r_P^{n+1}(n+3-\nu)}\iint_{\sigma}\left[\left(1+\frac{Z}{R}\right)^{n+3-\nu} - \left(1+\frac{H}{R}\right)^{n+3-\nu}\right]P_n\left(\cos\psi_{PQ}\right)d\sigma. \tag{7}$$

The two terms in square bracket can be expanded into a binomial series and eventually truncated, since the series is converging fast. In our investigation we consider the expansion to fourth order. Cf. Sun and Sjöberg (2001). Further simplifications yield

$$V_{ext}^a(P) = G\rho_0\sum_{n=0}^{\infty}\frac{R^{n+3}}{r_P^{n+1}}\iint_{\sigma}F(Q)P_n\left(\cos\psi_{PQ}\right)d\sigma, \tag{8}$$

where

$$F(Q) = \frac{Z-H}{R} + (n+2-\nu)\frac{Z^2-H^2}{2R^2} + (n+2-\nu)(n+1-\nu)\frac{Z^3-H^3}{6R^3}. \tag{9}$$

According to the addition theorem of the fully-normalized spherical harmonics

$$P_n\left(\cos\psi_{PQ}\right) = \frac{1}{2n+1}\sum_{m=-n}^{n} Y_{nm}(Q)Y_{nm}(P), \tag{10}$$

where $Y_{nm}(P)$ and $Y_{nm}(Q)$ are the spherical harmonics at any point P and Q and

$$\iint_{\sigma} Y_{nm}(Q)Y_{n'm'}(P)d\sigma = 4\pi\delta_{nn'}\delta_{mm'}, \tag{11}$$

where δ is Kronecker's delta, we have

$$V_{ext}^a(P) = 4\pi G\rho_0 R^2\sum_{n=0}^{\infty}\left(\frac{R}{r_P}\right)^{n+1}\frac{1}{2n+1}\sum_{m=-n}^{n}\left(F_{ext}^a\right)_{nm}Y_{nm}(P), \tag{12}$$

where

$$\left(F^{a}_{ext}\right)_{nm}=\frac{Z\delta_{n0}-H_{nm}}{R}+\left(n+2-\nu\right)\frac{Z^{2}\delta_{n0}-H^{2}{}_{nm}}{2R^{2}}+\left(n+2-\nu\right)\left(n+1-\nu\right)\frac{Z^{3}\delta_{n0}-H^{3}{}_{nm}}{6R^{3}}, \qquad (13)$$

where H_{nm}, $H^{2}{}_{nm}$ and $H^{3}{}_{nm}$ are the spherical harmonic coefficients of H, H^{2} and H^{3}, respectively derived in a global spherical harmonic analysis of topographic heights. Considering in Eq. (12) that

$$GM=4\pi\rho_{e}GR^{3}/3, \qquad (14)$$

where ρ_{e} =5500 kg/ m^{3} [Novák and Grafarend, 2006] is the mean density of the Earth, and M is the Earth's mass, we finally obtain

$$V^{a}_{ext}\left(P\right)=\frac{GM}{R}\sum_{n=0}^{\infty}\left(\frac{R}{r_{P}}\right)^{n+1}\sum_{m=-n}^{n}\left(v^{a}_{ext}\right)_{nm}Y_{nm}\left(P\right), \qquad (15)$$

where

$$\left(v^{a}_{ext}\right)_{nm}=\frac{3\rho_{0}}{(2n+1)\rho_{e}}\left(F^{a}_{ext}\right)_{nm}. \qquad (16)$$

Equation (16) represents the spherical harmonic coefficients of the external atmospheric potential. The above formula is analogous to that obtained by Novák and Grafarend (2006). The only difference is related to the ADM, which leads to the following harmonic coefficients in Novák and Grafarend (2006):

$$\left(F^{a}_{ext}\right)_{nm}=\frac{Z\delta_{n0}-H_{nm}}{R}+\left(n+2-\alpha R\right)\frac{Z^{2}\delta_{n0}-H^{2}{}_{nm}}{2R^{2}}+\left[\left(n+2\right)\left(n+1-2\alpha R\right)+2\beta R^{2}\right]\frac{Z^{3}\delta_{n0}-H^{3}{}_{nm}}{6R^{3}}$$

. (17)

It is now worth to compare Eq. (17) with Eq. (13). By comparing the second order terms in those equations, we observe that there is $\alpha R=-596.55$ in Novák and Grafarend's model, while we have $\nu=850$ in KTHA. Also, the coefficient of the third term in Eq. (13) can be written as $\left[\left(n+2\right)\left(n+1-\nu\right)-\left(n+1\right)\nu+\nu^{2}\right]$, and as one can see, an extra term appears vs. Novák and Grafarend's model. The constant terms of both formulas are not comparable as they are $2\beta R^{2}=226623.09$ and $\nu^{2}=722500$. However when the terms are divided by $6R^{3}$ the effect of the third term is considerably reduced. In comparison with Sjöberg (1998), we can say that, since Sjöberg's emphasis was on the DAE of the gravity anomaly and geoid, the upper limit of the radial integral in Eq. (4) was set to infinity, and the internal type of Legendre expansion was used instead of Eq. (5), but in our case that we want to obtain the DAE on the SGG data we have to limit this upper bound to the specific value r_{z} =6628137 m. It means that we assume the massive part of the atmosphere is below r_{z} level from the Earth's mean sphere. It is also possible to consider the satellite elevation as this specific value.

Now, consider the computation point to be below the atmospheric masses, in such a case the internal atmospheric potential should be formulated. Similar to the external atmospheric

potential formulation in spherical harmonics, we start with the Newtonian volume integral, Eq. (4) and consider Eq. (1) as the ADM (KTHA). If we expand the $1/l_{PQ}$ into Legendre series of internal type

$$\frac{1}{l_{PQ}} = \frac{1}{r_P}\sum_{n=0}^{\infty}\left(\frac{r_P}{r_Q}\right)^{n+1} P_n\left(\cos\psi_{PQ}\right), \tag{18}$$

and put it back into Eq. (4), after some further simplifications we have

$$V_{int}^{a}\left(P\right) = G\sum_{n=0}^{\infty}\rho_0 R^{\nu} r_P^n \iint_{\sigma}\int_{r_S}^{r_Z} r_Q^{1-n-\nu} dr_Q P_n\left(\cos\psi_{PQ}\right)d\sigma . \tag{19}$$

In a similar way as for the external atmospheric potential we obtain

$$V_{int}^{a}\left(P\right) = G\rho_0\sum_{n=0}^{\infty}\frac{-R^{-n+2}r_P^n}{\left(n+\nu-2\right)}\iint_{\sigma}\left[\left(1+\frac{Z}{R}\right)^{-\left(n+\nu-2\right)} - \left(1+\frac{H}{R}\right)^{-\left(n+\nu-2\right)}\right]P_n\left(\cos\psi_{PQ}\right)d\sigma . \tag{20}$$

If the two terms in the square bracket are expanded into a binomial series up to fourth order, after some simplifications we obtain

$$V_{int}^{a}\left(P\right) = G\rho_0\sum_{n=0}^{\infty}\frac{R^{-n+2}r_P^n}{2n+1}\sum_{m=-n}^{n}\iint_{\sigma}F_{int}^{a}\left(Q\right)Y_{nm}\left(Q\right)d\sigma Y_{nm}\left(P\right), \tag{21}$$

where

$$F_{int}^{a}\left(Q\right) = \frac{Z-H}{R} - \left(n+\nu-1\right)\frac{\left(Z^2-H^2\right)}{2R^2} + \left(n+\nu-1\right)\left(n+\nu\right)\frac{\left(Z^3-H^3\right)}{6R^3} . \tag{22}$$

Again, spherical harmonic expansion of H and Z yields

$$V_{int}^{a}\left(P\right) = 4\pi G\rho_0 R^2\sum_{n=0}^{\infty}\frac{1}{2n+1}\left(\frac{r_P}{R}\right)^n\sum_{m=-n}^{n}\left(F_{int}^{a}\right)_{nm}Y_{nm}\left(P\right), \tag{23}$$

where

$$\left(F_{int}^{a}\right)_{nm} = \left\{\frac{Z\delta_{n0}-H_{nm}}{R} - \frac{\left(n+\nu-1\right)}{2R^2}\left(Z^2\delta_{n0}-H^2{}_{nm}\right) + \frac{\left(n+\nu-1\right)\left(n+\nu\right)}{6R^3}\left(Z^3\delta_{n0}-H^3{}_{nm}\right)\right\}, \tag{24}$$

and according to Eq. (14), we finally arrive at

$$V_{int}^{a}\left(P\right) = \frac{GM}{R}\sum_{n=0}^{\infty}\left(\frac{r_P}{R}\right)^n\sum_{m=-n}^{n}\left(v_{int}^{a}\right)_{nm}Y_{nm}\left(P\right), \tag{25}$$

where

$$\left(v_{int}^{a}\right)_{nm} = \frac{3\rho_0}{\left(2n+1\right)\rho_e}\left(F_{int}^{a}\right)_{nm} . \tag{26}$$

This derivation is comparable with that obtained by using the NADM for the internal atmospheric potential in spherical harmonics yielding [Eshagh and Sjöberg, submitted]

$$\left(F_{int}^{a}\right)_{nm}=\frac{Z\delta_{n0}-H_{nm}}{R}-\left(n-1-\alpha R\right)\frac{Z^{2}\delta_{n0}-H^{2}{}_{nm}}{2R^{2}}-\left[\left(1-n\right)\left(n+2\alpha R\right)-2\beta R^{2}\right]\frac{Z^{3}\delta_{n0}-H^{3}{}_{nm}}{6R^{3}}. \tag{27}$$

Novák (2000) proposed to use atmospheric shells with different densities (based on the USSA76) for generating the atmospheric potential between 10 and 86 km levels. The potential of such atmospheric shells can be considered as an additional value to the zero-degree harmonic coefficient; see Novák (2000). On the contrary, there is no restriction in elevation for the KTHA, and it can theoretically be considered up to infinity. However the approximations used in generating the atmospheric potential may not be accurate enough for higher elevations based on this model. As Z in Eq. (9) is a constant it only contributes to the zero-degree harmonic. It is obvious that when increasing the elevation of the upper boundary of the atmosphere, the magnitude of this harmonic can increase unboundedly. In order to solve this problem we propose to use the following relation for the zero-degree harmonic coefficient of the atmospheric potential (which follows from Eq. 6 for n=0).

$$\left(v_{ext}^{a}\right)_{0}=\frac{3\rho_{0}}{\rho_{e}\left(3-\nu\right)}\left\{\left(1+\frac{Z}{R}\right)^{3-\nu}-\bar{H}\right\}, \tag{28}$$

where

$$\bar{H}=\frac{1}{4\pi}\iint_{\sigma}\left(1+\frac{H}{R}\right)^{3-\nu}d\sigma. \tag{29}$$

The integral of Eq.(29) can be solved numerically.

4. Atmospheric potential based on the NKTHA

Now we consider the NKTHA that we proposed in Section 2.3. This model is a combination of the NADM and the KTHA. In the following we express how to use this NKTHA for formulating the external and internal atmospheric potentials in spherical harmonics.

Inserting the NKTHA into Eq. (4) and considering Eq. (3) and the external type of expansion of $1/l_{PQ}$ we obtain

$$V_{ext}^{a}\left(P\right)=G\sum_{n=0}^{\infty}\frac{1}{r_{P}^{n+1}}\iint_{\sigma}\left[\int_{r_{S}}^{H_{0}}\rho^{a}\left(r_{Q}\right)r_{Q}{}^{n+2}dr_{Q}+\int_{H_{0}}^{r_{Z}}\rho^{a}\left(r_{Q}\right)r_{Q}{}^{n+2}dr_{Q}\right]P_{n}\left(\cos\psi_{PQ}\right)d\sigma. \tag{30}$$

The ADM in the first integral in the square bracket is related the upper function of Eq.(3) and the second integral relates to the lower function. Therefore the solution of the first term is the same as in Eq. (17). Considering the second part of Eq. (3) as the ADM above H_0, the solution of the second integral becomes

$$\rho\left(H_{0}\right)\left(R+H_{0}\right)^{\nu}\int_{R+H_{0}}^{R+Z}r_{Q}{}^{n+2-\nu}dr_{Q}=\frac{\rho\left(H_{0}\right)R^{n+3}}{n+3-\nu}\left[\left(1+\frac{H_{0}}{R}\right)^{\nu}\left(1+\frac{Z}{R}\right)^{n+3-\nu}-\left(1+\frac{H_{0}}{R}\right)^{n+3}\right],$$

(31)

Since this term is a constant w.r.t integration point Q in Eq. (31), it associates just with the zero-degree harmonic. The unitless spherical harmonic coefficients of the external atmospheric potential can thus be written in the following form

$$\left(v_{ext}^{a}\right)_{nm}=\frac{3}{(2n+1)\rho_e}\left(\rho_0\left(F_{ext}^{a}\right)_{nm}+\rho(H_0)G_n\right), \tag{32}$$

where $\left(F_{ext}^{a}\right)_{nm}$ was defined in Eq. (17), and

$$G_n=\frac{1}{n+3-\nu}\left[\left(1+\frac{H_0}{R}\right)^{\nu}\left(1+\frac{Z}{R}\right)^{n+3-\nu}-\left(1+\frac{H_0}{R}\right)^{n+3}\right]\delta_{n0}. \tag{33}$$

Inserting Eqs. (33) and (17) into Eq. (32) and setting $Z\delta_{n0}=H_0\delta_{n0}$ we have

$$\left(V_{ext}^{a}\right)_{nm}=\frac{3}{(2n+1)\rho_e}\left\{\rho_0\left[\frac{H_0\delta_{n0}-H_{nm}}{R}+(n+2-\alpha R)\frac{H_0^2\delta_{n0}-H^2{}_{nm}}{2R^2}+\left[(n+2)(n+1-2\alpha R)+\right.\right.\right.$$
$$\left.\left.\left.+2\beta R^2\right]\frac{H_0^3\delta_{n0}-H^3{}_{nm}}{6R^3}+\frac{\rho(H_0)}{n+3-\nu}\left[\left(1+\frac{H_0}{R}\right)^{\nu}\left(1+\frac{Z}{R}\right)^{n+3-\nu}-\left(1+\frac{H_0}{R}\right)^{n+3}\right]\delta_{n0}\right\}, \tag{34}$$

For generating the external atmospheric potential based on the NKTHA it is sufficient just to insert the harmonic coefficients generated according to Eq. (34) into Eq. (15).

We can also consider our new atmospheric model NKTHA to generate the internal type of the atmospheric potential. By considering Eq. (18) and Eq. (3) (the NKTHA) and reinserting into Eq. (4) we obtain

$$V_{int}^{a}(P)=G\sum_{n=0}^{\infty}r_P^n\left[\int_{r_S}^{H_0}\rho^a(r_Q)\,r_Q{}^{-n+1}dr_Q+\int_{H_0}^{r_Z}\rho^a(r_Q)\,r_Q{}^{-n+1}dr_Q\right]P_n\left(\cos\psi_{PQ}\right)d\sigma. \tag{35}$$

The first integral in the square bracket is the same as in the internal type of the NADM and is also the same as Eq. (27). The second part can be written

$$\rho(H_0)(R+H_0)^{\nu}\int_{R+H_0}^{R+Z}r_Q{}^{-n+1-\nu}dr_Q=\frac{\rho(H_0)R^{-n+2}}{-n-\nu+2}\left[\left(1+\frac{H_0}{R}\right)^{\nu}\left(1+\frac{Z}{R}\right)^{-n-\nu+2}-\left(1+\frac{H_0}{R}\right)^{-n+2}\right], \tag{36}$$

and the harmonic coefficients of the internal atmospheric potential can thus be written

$$\left(v_{int}^{a}\right)_{nm}=\frac{3}{(2n+1)\rho_e}\left(\rho_0\left(F_{int}^{a}\right)_{nm}+\rho(H_0)K_n\right), \tag{37}$$

where $\left(F^{a}_{int}\right)_{nm}$ is the same as in Eq. (27) and

$$K_n = \frac{1}{-n-v+2}\left[\left(1+\frac{H_0}{R}\right)^{v}\left(1+\frac{Z}{R}\right)^{-n-v+2} - \left(1+\frac{H_0}{R}\right)^{-n+2}\right]\delta_{n0}. \quad (38)$$

Finally we obtain

$$\left(V^{a}_{int}\right)_{nm} = \frac{3}{(2n+1)\rho_e}\left\{\rho_0\left[\frac{H_0\delta_{n0}-H_{nm}}{R} - (n-1-\alpha R)\frac{H^2{}_0\delta_{n0}-H^2{}_{nm}}{2R^2} - \left[(1-n)(n+2\alpha R)-2\beta R^2\right]\times\right.\right.$$
$$\left.\left.\times\frac{H^3{}_0\delta_{n0}-H^3{}_{nm}}{6R^3}\right] + \frac{\rho(H_0)}{-n-v+2}\left[\left(1+\frac{H_0}{R}\right)^{v}\left(1+\frac{Z}{R}\right)^{-n-v+2} - \left(1+\frac{H_0}{R}\right)^{-n+2}\right]\delta_{n0}\right\}. \quad (39)$$

It should be noted that these harmonic coefficients should be inserted into Eq. (25) for generating the internal atmospheric potential.

5. DAE on the SGG data

According to the spherical harmonic coefficients of the external atmospheric potential, the DAE can easily be computed by putting the harmonic coefficients into the spherical harmonic expansion of the SGG data either in a geocentric spherical, local, or orbital frame. In our study we use the orbital frame to present the effects. The non-singular expression of the gradients in this frame is preferrable for us, as we do not have to compute the associated Legendre function derivatives. These formulas were originally presented by Petrovskaya and Vershkov (2006). The orbital frame is defined by u, v and w axes so that w axis coincides with z and upward, v points towards the instantaneous angular momentum vector and u complements the right-handed triad. The mathematical models of the SGG data in such a frame are presented as follows [Petrovskaya and Vershkov, 2006]:

$$V_{uu}(P) = \frac{GM}{R^3}\sum_{n=2}^{N}\sum_{m=-n}^{n}\left(\frac{R}{r_P}\right)^{n+3}\left(v^{a}_{ext}\right)_{nm}\left\{Q_m(\lambda_P)\left[\cos 2\alpha f_{n,m,1} - \cos^2\alpha(n+1)(n+2)\bar{P}_{n,|m|}\right] + \right.$$
$$\left. + Q_{-m}(\lambda_P)\sin 2\alpha f_{nm,2}\right\} \quad (40)$$

$$V_{vv}(P) = -\frac{GM}{R^3}\sum_{n=2}^{N}\sum_{m=-n}^{n}\left(\frac{R}{r_P}\right)^{n+3}\left(v^{a}_{ext}\right)_{nm}\left\{Q_m(\lambda_P)\left[\cos 2\alpha f_{nm,1} + \sin^2\alpha(n+1)(n+2)\bar{P}_{n,|m|}\right] + \right.$$
$$\left. + Q_{-m}(\lambda_P)\sin 2\alpha f_{nm,2}\right\} \quad (41)$$

$$V_{uv}(P) = -\frac{GM}{R^3}\sum_{n=2}^{N}\sum_{m=-n}^{n}\left(\frac{R}{r_P}\right)^{n+3}\left(v^{a}_{ext}\right)_{nm}\left\{Q_m(\lambda_P)\left[\sin 2\alpha f_{nm,1} - \cos\alpha\sin\alpha(n+1)(n+2)\bar{P}_{n,|m|}\right] + \right.$$
$$\left. - Q_{-m}(\lambda_P)\cos 2\alpha f_{nm,2}\right\} \quad (42)$$

$$V_{uw}(P) = \frac{GM}{R^3}\sum_{n=2}^{N}\sum_{m=-n}^{n}\left(\frac{R}{r_P}\right)^{n+3}\left(v^{a}_{ext}\right)_{nm}\left[Q_m(\lambda_P)\cos\alpha f_{nm,3} + Q_{-m}(\lambda_P)\sin\alpha f_{nm,4}\right] \quad (43)$$

$$V_{vw}(P) = -\frac{GM}{R^3}\sum_{n=2}^{N}\sum_{m=-n}^{n}\left(\frac{R}{r_P}\right)^{n+3}\left(v^{a}_{ext}\right)_{nm}\left[Q_m(\lambda_P)\sin\alpha f_{nm,3} - Q_{-m}(\lambda_P)\cos\alpha f_{nm,4}\right] \quad (44)$$

$$V_{ww}(P)=\frac{GM}{R^3}\sum_{n=2}^{N}\sum_{m=-n}^{n}(n+1)(n+2)\left(\frac{R}{r_P}\right)^{n+3}\left(v_{ext}^{a}\right)_{nm}Q_m(\lambda_P)\bar{P}_{n,|m|} \tag{45}$$

where, $\bar{P}_{n,|m|}=\bar{P}_{n,|m|}(\cos\theta_P)$ and $f_{nm,1}=f_{nm,1}(\theta_P)$

$$f_{nm,1}(\theta_P)=a_{nm}\bar{P}_{n,|m|-2}+b_{nm}\bar{P}_{n,|m|}+c_{nm}\bar{P}_{n,|m|+2}, \tag{46}$$

$$f_{nm,2}(\theta_P)=d_{nm}\bar{P}_{n-1,|m|-2}+g_{nm}\bar{P}_{n-1,|m|}+h_{nm}\bar{P}_{n-1,|m|+2}, \tag{47}$$

$$f_{nm,3}(\theta_P)=\beta_{nm}\bar{P}_{n,|m|-1}+\gamma_{nm}\bar{P}_{n,|m|+1}, \tag{48}$$

$$f_{nm,4}(\theta_P)=\mu_{nm}\bar{P}_{n-1,|m|-1}+\nu_{nm}\bar{P}_{n-1,|m|+1}, \tag{49}$$

$$Q_m(\lambda_P)=\begin{cases}\cos m\lambda_P & m\geq 0\\ \sin|m|\lambda_P & m<0\end{cases} \tag{50}$$

where, $\left(v_{ext}^{a}\right)_{nm}$ is the spherical harmonic coefficients of the external atmospheric potential, θ_P and λ_P and r_P are the co-latitude, longitude and geocentric radius of the point P or the satellite position. N is the maximum degree of harmonic expansion, and $\bar{P}_{n,|m|}$ is the fully-normalized associated Legendre function of degree n and order m. α is the satellite track azimuth. a_{nm}, b_{nm}, c_{nm}, d_{nm}, g_{nm}, h_{nm}, β_{nm}, γ_{nm}, μ_{nm} and ν_{nm} are the constant coefficients presented in Appendix B.

These formulas were generally designed for gravitational gradients of the disturbing potential. We can include the effect of zero- and first-harmonics separately. The contribution of these harmonics is presented in Appendix C.

6. Remote-Compute-Restore scheme

In the remove-compute-restore approach, the external topographic and atmospheric potentials are removed and the result will be no-topography and no-atmosphere potentials. The effect of the topographic and atmospheric masses must be restored after computations (this is why the method is called remove-compute-restore). The gravity field can also be determined locally from SGG data using inversion of the second order derivatives of extended Stokes or Abel-Poisson integrals. The downward continued gravity anomaly or disturbing potential at sea level is the results of this inversion process. One can also downward continue the SGG data directly to geoid height or gravity anomaly at sea level. In any case, the effect of the removed atmospheric potential should be restored on these quantities. In the following we present these indirect atmospheric effects on the gravity anomaly and geoid height.

According to the fundamental equation of physical geodesy we have [Heiskanen and Moritz, 1967, p. 86]:

$$\delta\Delta g_{ind}^{a}(P)=-\frac{\partial V_{int}^{a}(P)}{\partial r_P}-\frac{2}{r_P}V_{int}^{a}(P). \tag{51}$$

$\delta\Delta g^{a}_{ind}(P)$ is the indirect atmospheric effect on gravity anomaly which should be restored. By putting the internal atmospheric potential given by Eq. (25) we obtain

$$\delta\Delta g^{a}_{ind}(P) = -\frac{GM}{R^2}\sum_{n=0}^{N}(n+2)\left(\frac{r_P}{R}\right)^{n-1}\sum_{m=-n}^{n}\left(v^{a}_{int}\right)_{nm}Y_{nm}(P), \tag{52}$$

and at the very approximate geoid $r_P = R$ we have

$$\delta\Delta g^{a}_{ind}(P) = -\frac{GM}{R^2}\sum_{n=0}^{N}(n+2)\sum_{m=-n}^{n}\left(v^{a}_{int}\right)_{nm}Y_{nm}(P). \tag{53}$$

The indirect atmospheric effect on the geoid will be

$$\delta N^{a}_{ind}(P) = -\frac{GM}{R\gamma}\sum_{n=0}^{N}\sum_{m=-n}^{n}\left(v^{a}_{int}\right)_{nm}Y_{nm}(P). \tag{54}$$

7. Numerical studies

Let us start with a simple investigation of the mathematical models approximating the atmospheric density. First we compare the NADM and KTHA with the USSA76 up to 86 km elevation (which is the maximum level of the USSA76). In the following figures, these approximating density models are visualized with respect to the elevation

Figure 1

Figure 1 shows that the NADM is valid up to 10 km elevation above sea level; see Novák (2001). The KTHA agrees with the USSA76 more or less but underestimates the atmospheric density below 20 km and overestimates it in higher altitudes. It should be mentioned that the main aim of Novák (2000) was to formulate the atmospheric topography. This is why he considered a simple polynomial to model the atmospheric density up to 10 km. Since 80% of atmospheric masses are below 12 km [Lambeck 1988], it is reasonable to use a simple polynomial to express the effect of atmospheric roughness although Wallace and Hobbs (1977) believes that 99% of the masses lie within the lowest 30 km above sea level.

For investigating the DAE on the SGG data, we generate the external atmospheric potential coefficients considering Z=10 km using both the NADM and the KTHA. The orbital frame is used to generate the DAE at 250 km level with 2-months revolution of the GOCE satellite over Fennoscandia. The position of the satellite can be generated using a numerical integration technique and an existing geopotential model. For more details the reader is referred to e.g., Hwang and Lin (1998), Eshagh (2003), Eshagh (2005) and Eshagh and Najafi-Alamdari (2006). The statistics of the computations are summarized in Table 1.

Table 1

It illustrates that the DAE on the SGG data is dependent on the ADM. The KTHA shows small DAE since it underestimates the massive part of the atmosphere in the lower altitudes. This underestimation of the atmospheric density directly affects the zero-degree harmonic coefficient of the atmospheric potential. Since V_{uu}, V_{vv} and V_{ww} include this harmonic in their formulation, we can expect to see larger DAE based on the NADM than the KTHA. V_{uv}, V_{uw} and V_{vw} are more or less in the same order in both approaches because of their independency from the zero-degree harmonic. However, it should be noted that V_{uw} and V_{vw} include also the first-degree harmonics.

The following figure shows more details about the behaviour of the zero-degree harmonic with respect to elevation.

Figure 2

Figure 2 illustrates values of the zero-degree harmonic based on the NADM and KTHA. As we know the NADM is valid just up to 10 km height, and it is not surprising to see larger values when applying it for the external potential to higher elevations. The horizontal line presented in the figure is the true value of the zero-degree harmonic computed by Eq. (28). As it is expected, this harmonic should be treated as a bounded function when increasing the elevation. However, Figure 2a shows that the approximations of the true mathematical expressions with binomial expansion which was used in Eq. (13) is good just for elevations lower than 20 km. The zero-degree harmonic has smaller value up to 50 km when KTHA is used vs. the NADM, while it is larger at 250km. It means that the approximation used Eq. (13) is not good enough for higher elevations and can destroy the solution even worse than the NADM see Figure 2a. The simplest way to get a non-diverging value for the zero-degree harmonic is to avoid approximations in this harmonic in the KTHA using Eq. (53). As we mentioned previously we can consider the atmospheric shells above 10 km and compute the atmospheric potential corresponding to each shell and add it in this harmonic; see Novák (2000).

The next point of our discussion is to consider a possible improvement of KTHA model. As we explained before the KTHA was derived using the results of Ecker and Mittermayer (1969) and USSA61 but the NADM is based on the USSA76. The difference between these two models is due to the differences in the original data used; see Table 2.

Table 2

Figure 1 shows that the KTHA are not well-fitted to the USSA76. Assuming the densities generated by the USSA76 as true values, we can modify the KTHA to obtain better fit to the USSA76. In Figures 3a and 3b results of this modification to the KTHA is presented.

Figure 3

By fitting the KTHA to the USSA76 we obtain the value $\nu \doteq 930$. This modified KTHA is visualized in Figure 3a, which figure shows that, although the modified KTHA has very good fit to the USSA76 in higher elevations, it underestimates the density of the most massive part of the atmosphere in low levels. Therefore it is expected to see small DAE on the SGG data. In Table 3 the statistics of these DAE based on the KTHA and the modified KTHA over Fennoscandia are presented.

Table 3

The differences are again mainly related to the diagonal elements V_{uu}, V_{vv} and V_{ww} of the gradiometric tensor as they, unlike the other elements, include the zero-degree harmonic. The difference between the DAEs generated based on the original and modified KTHA is related to the underestimation of the atmospheric density in the modified KTHA and also to significant overestimation of KTHA in higher elevation. However, since the most massive part of the atmosphere lies below 10 km level we can expect that the underestimation of the atmospheric density in the modified KTHA is the main reason for these differences. The only advantage of the modified KTHA relative to the original KTHA is thus to have a better fit in the higher elevations. Consequently, the modified KTHA is inferior to the original KTHA in context of the gravimetric data processing.

We also consider another approach in which the NADM is used for the heights below 10 km and another modified KTHA for considering higher levels. In this case the atmospheric density generated by the NADM at 10 km is considered as a reference value and the KTHA model is modified to get best fit to the densities of the USSA76 after 10 km. Figure 3b shows the result of this fitting. The figure shows that the atmospheric densities are overestimated by the NKTHA with respect to the USSA76 between 20 and 60 km levels. However since the atmospheric density decreases fast by increasing the elevation we can expect that such misfitness is insignificant in higher levels. In this case we estimate $\nu'' = 890.1727 \doteq 890$, see Eq. (3). The RMSEs of the model fittings are 0.038, 0.032 and 0.0027 kg/m^3 for KTHA, modified KTHA and new KTHA, respectively.

In Table 4 the statistics of the DAE on the SGG data over Fennoscandia are presented based on the NKTHA.

Table 4

Since in the NKTHA we use the NADM for the elevations below 10 km, we expect to see a good fit to the DAE for these ADMs, which is confirmed by the statistics in Tables 1 and 4.

In the following we present the maps of the DAE on the SGG data over Fennoscandia. In order to simulate the satellite orbit the 4-th order Runge-Kutta integrator was used to integrate the satellite accelerations generated from EGM96 geopotential model to degree 360. Two-month revolution of the satellite with 30 second integration step size was considered in our investigation over Fennoscandia. The lower boundary of the atmosphere was considered the Earth surface and the upper bound at satellite level. The JGP95e global topographic model was also used to generate the topographic harmonics to degree and order 360.

Figure 4

Figure 4 illustrates the DAE on the SGG data at 250km based on the NKTHA. (a), (b), (c), (d), (e) and (f) are V_{uu}, V_{vv}, V_{ww}, V_{uv}, V_{uw} and V_{vw}, respectively. The largest DAE is about 5.1381 mE and related to V_{ww} as would we expect, and the smallest DAE (about -0.0276 mE) is related to V_{uv}.

The numerical results show that the DAE on the SGG data based on all ADMs is at mE level. Such effects are significant in precise validation of the SGG data. On the other hand, Xu (1992, 1998) and Xu and Rummel (1994) concluded that in inverting the SGG data for the determination of the local gravity anomaly at the mean sphere of the Earth with 5 mGal level of accuracy, 0.01E accuracy for the SGG data is enough. Hence if such an accuracy for gravity anomaly be required one can safely ignore the DAE on the SGG data. It should be mentioned that the atmospheric effect is also highly variable in time, which would have to be taken into account in future gradiometric missions.

8. Conclusions

The KTH atmospheric density model (KTHA) was modified so that it delivers better fit to the United States atmospheric density model (USSA76) than the original one (which was derived based on the United States atmospheric density model presented in 1961, USSA61), and the constant ν=930 was obtained for the modified model. Numerical studies show that this model underestimates the most massive part of the atmosphere which is below 10 km more than the original one, but it has better fit for higher elevations, and this effect on the satellite gravity gradiometry is less than 1mE and negligible. A combination of both density models presented by Novák (2000) and Sjöberg (1998) with a simple modification was proposed as a new model (NKTHA). This model has good fit with the USSA76 for low and high levels. The spherical harmonics coefficients of the atmospheric potential generated based on this new model were used to compute the DAEs on the SGG data in the orbital frame. Numerical results show that the maximum DAE is related to V_{ww} and about 5.13 mE. In comparison with Novák (2000) model, which generate the corresponding value 4.44 mE, one can state that the effect of the atmospheric masses above 10 km is less than 1 mE but significant for precise validation of the SGG. We recommend the use of NKTHA in considering atmospheric effects in satellite gradiometry data processing and any other gravimetric applications.

Acknowledgment

The Swedish National Space Board (SNSB) is cordially acknowledged for its financial support. The first author would like to thank Prof. P. Novák for the stimulating discussions about atmospheric effect. Also we appreciate the thorough work of the two reviewers, with many detailed remarks, that helped in making the paper more understandable.

Appendix A

The constant coefficients related to Eqs. (40)-(45) are [Petrovskaya and Vershkov 2006]:

$$a_{nm}=\begin{cases}0 & |m|=0,1\\ \frac{\sqrt{1+\delta_{|m|,2}}}{4}\sqrt{n^2-(|m|-1)^2}\sqrt{n+|m|}\sqrt{n-|m|+2} & 2\le|m|\le n\end{cases} \quad (A.1)$$

$$b_{nm}=\begin{cases}\frac{(n+|m|+1)(n+|m|+2)}{2(|m|+1)} & |m|=0,1\\ \frac{n^2+m^2+3n+2}{2} & 2\le|m|\le n\end{cases} \quad (A.2)$$

$$c_{nm}=\begin{cases}\frac{\sqrt{1+\delta_{|m|,0}}}{4}\sqrt{n^2-(|m|+1)^2}\sqrt{n-|m|}\sqrt{n+|m|+2}, & |m|=0,1\\ \frac{1}{4}\sqrt{n^2-(|m|+1)^2}\sqrt{n-|m|}\sqrt{n+|m|+2}, & 2\le|m|\le n\end{cases} \quad (A.3)$$

$$d_{nm}=\begin{cases}0 & |m|=1\\ -\frac{m}{4|m|}\sqrt{\frac{2n+1}{2n-1}}\sqrt{1+\delta_{|m|,2}}\sqrt{n^2-(|m|-1)^2}\sqrt{n+|m|}\sqrt{n+|m|-2}, & 2\le|m|\le n\end{cases} \quad (A.4)$$

$$g_{nm}=\begin{cases}\frac{m}{4|m|}\sqrt{\frac{2n+1}{2n-1}}\sqrt{n+1}\sqrt{n-1}(n+2), & |m|=1\\ \frac{m}{2}\sqrt{\frac{2n+1}{2n-1}}\sqrt{n+|m|}\sqrt{n-|m|}, & 2\le|m|\le n\end{cases} \quad (A.5)$$

$$h_{nm}=\begin{cases}\frac{m}{4|m|}\sqrt{\frac{2n+1}{2n-1}}\sqrt{n-3}\sqrt{n-2}\sqrt{n-1}\sqrt{n+2}, & |m|=1\\ \frac{m}{4|m|}\sqrt{\frac{2n+1}{2n-1}}\sqrt{n^2-(|m|+1)^2}\sqrt{n-|m|}\sqrt{n-|m|-2}, & 2\le|m|\le n\end{cases} \quad (A.6)$$

$$\beta_{nm}=\begin{cases}0 & |m|=0\\ \frac{n+2}{2}\sqrt{1+\delta_{|m|,1}}\sqrt{n+|m|}\sqrt{n-|m|+1}, & 1\le|m|\le n\end{cases} \quad (A.7)$$

$$\gamma_{nm}=\begin{cases}-(n+2)\sqrt{\frac{n(n+1)}{2}}, & |m|=0\\ -\frac{(n+2)}{2}\sqrt{n-|m|}\sqrt{n+|m|+1}, & 1\le|m|\le n\end{cases} \quad (A.8)$$

$$\mu_{nm}=-\frac{m}{|m|}\left(\frac{n+2}{2}\right)\sqrt{\frac{2n+1}{2n-1}}\sqrt{1+\delta_{|m|,1}}\sqrt{n+|m|}\sqrt{n+|m|-1} \quad (A.9)$$

$$v_{nm} = -\frac{m}{|m|}\left(\frac{n+2}{2}\right)\sqrt{\frac{2n+1}{2n-1}}\sqrt{n-|m|}\sqrt{n-|m|-1} \qquad \text{(A. 10)}$$

where δ is Kronecker's delta.

Appendix B

The contribution of the zero- and the first-degree harmonics to Eqs (40)-(45) can be derived based on the original formulas of the gravitational gradients in the orbital frame as (see also Petrovskaya and Vershkov 2006, Eq. 45):

$$V_{uu}^{0,1}(P) = V_{xx}^{0,1}(P) = -\frac{GMR}{r_P^4}\left\{\frac{r_P}{R}C_{00} + 3\sqrt{3}\left[C_{10}\cos\theta_P + \left(C_{11}\cos\lambda_P + S_{11}\sin\lambda_P\right)\sin\theta_P\right]\right\}, \text{(B.1)}$$

$$V_{vv}^{0,1}(P) = V_{yy}^{0,1}(P) = -\frac{GMR}{r_P^4}\left\{\frac{r_P}{R}C_{00} + 3\sqrt{3}\left[C_{10}\cos\theta_P + \left(C_{11}\cos\lambda_P + S_{11}\sin\lambda_P\right)\sin\theta_P\right]\right\}, \text{(B.2)}$$

$$V_{ww}^{0,1}(P) = V_{zz}^{0,1}(P) = \frac{2GMR}{r_P^4}\left\{\frac{r_P}{R}C_{00} + 3\sqrt{3}\left[C_{10}\cos\theta_P + \left(C_{11}\cos\lambda_P + S_{11}\sin\lambda_P\right)\sin\theta_P\right]\right\}, \text{(B.3)}$$

$$V_{uv}^{0,1}(P) = V_{xy}^{0,1}(P) = 0, \qquad \text{(B.4)}$$

$$V_{uw}^{0,1}(P) = \frac{3\sqrt{3}GMR}{r_P^4}\left\{\cos\alpha\left[C_{10}\sin\theta_P + \left(C_{11}\cos\lambda_P + S_{11}\sin\lambda_P\right)\cos\theta_P\right] + \right.$$
$$\left. + \sin\alpha\left(-C_{11}\sin\lambda_P + S_{11}\cos\lambda_P\right)\right., \qquad \text{(B.5)}$$

$$V_{vw}^{0,1}(P) = \frac{3\sqrt{3}GMR}{r_P^4}\left\{-\sin\alpha\left[-C_{10}\sin\theta_P + \left(C_{11}\cos\lambda_P + S_{11}\sin\lambda_P\right)\cos\theta\right] + \right.$$
$$\left. + \cos\alpha\left(-C_{11}\sin\lambda_P + S_{11}\cos\lambda_P\right)\right., \qquad \text{(B.6)}$$

where superscripts of 0 and1 stand for the zero- and the first-degree harmonics, respectively. C_{00}, C_{10}, C_{11}, S_{10} and S_{11} are the fully-normalized zero- and the first-degree geopotential coefficients.

References

Albertella A, F. Migliaccio, F. Sansò (2002). GOCE: The earth field by space gradiometry, Celestial Mechanics and Dynamical Astronomy 83:1-15. doi: 10.1023/A:1020104624752

Anderson EG., and Mather RR. (1975) Atmospheric effects in physical geodesy. Unisurv G23:23-41, University of NSW, Sydney, Australia

Balmino G., F. Perosanz, R. Rummel, N. Sneeuw, H. Sünkel, P. Woodworth (1998). European Views on Dedicated Gravity Field Missions: GRACE and GOCE, An Earth Sciences Division Consultation Document, ESA, ESD-MAG-REP-CON-001.

Balmino G., F. Perosanz, R. Rummel, N. Sneeuw and H. Suenkel (2001). CHAMP, GRACE and GOCE: Mission concepts and cimulations. Bollettino di Geofisica Teoricae Applicata, 40, 3-4, 309-320.

Ecker E. and Mittermayer E. (1969) Gravity corrections for the influence of the atmosphere. Bollettino di Geofisica Teorica ed Applicata, 11:70-80

ESA (1999). Gravity field and steady-state ocean circulation mission, ESA SP-1233(1), Report for mission selection of the four candidate earth explorer missions, ESA Publications Division, pp. 217, July 1999.

Eshagh M. (2003) Precise orbit determination of low Earth orbiting satellite, Msc thesis, Department of Geodesy and Geomatics, K.N.Toosi University of Technology, Tehran, Iran

Eshagh M. (2005) Step-variable numerical orbit integration of a low Earth orbiting satellite, Journal of the Earth & Space Physics, Vol. 31, No. 1, 2005, pp. 1-12

Eshagh M. and Najafi-Alamdari M. (2006) Comparison of numerical Integration methods in orbit determination of low earth orbiting satellites, Journal of the Earth & Space Physics Vol. 32, No. 3, pp. 41-57

F. Flechtner, R. Schmidt, and U. Meyer. De-aliasing of short-term atmospheric and oceanic mass variations for GRACE. In J. Fluty, R. Rummel, C. Reigber, M. Rotacher, G. Boedeker, and U. Schreiber, editors, Observation of the Earth system from space, pages 189-214. Springer, Berlin, Heidelberg, 2006.

Heck, B. (2003) On Helmert's Methods of Condensation. Journal of Geodesy, vol 77:155-170. doi: 10.1007/s00190-003-0318-5

Heiskanen W. and Moritz H. (1967) Physical geodesy. W.H. Freeman, San Francisco

Hwang, C., and Lin J.M. (1998) Fast integration of low orbiter's trajectory perturbed by the earth's non-sphericity, Journal of Geodesy, 72:578-585, doi: 10.1007/s001900050196

Lambeck K., (1988) Geophysical geodesy, the slow deformations of the Earth. Clarendon, Oxford University Press, New York

Makhloof A. and Ilk K.H. (2005) Far-zone topography effects on gravity and geoid heights according to Helmert's methods of condensation and based on Airy-Heiskanen model, proceedings the 3rd minia International conference for advanced trends in Engineering, El-Minia, April 3-5, 2005.

Makhloof, A. and Ilk, K. H. (2006) Band-limited topography effects in airborne gravimetry using space localizing base functions, EGU conference, 3 April, 2006

Makhloof A. (2007) The use of topographic-isostatic mass information in geodetic applications, Doctoral dissertation, Department of Theoretical and Physical Geodesy, Bonn, Germany

Martinec Z., Matyska C., Grafarend E.W. and Vaníček P. (1993) On Helmert's 2nd condensation method, Manuscripta Geodaetica, 18:417-421

Martinec Z. and Vaníček P. (1994) Direct topographical effect of Helmert's condensation for a spherical geoid. Manuscripta Geodaetica, 19: 257-268

Moritz H. (1980) Advanced physical geodesy. Herbert Wichman, Karlsruhe

Nahavandchi H. (2004) A new strategy for the atmospheric gravity effect in gravimetric geoid determination, Journal of Geodesy, 77:823-828, doi: 10.1007/s00190-003-0358-x

Novák P. (2000) Evaluation of gravity data for the Stokes-Helmert solution to the geodetic boundary-value problem, Technical report 207, Department of Geodesy and Geomatics Engineering, University of New Brunswick, Fredericton, Canada

Novák P. and Grafarend W.E. (2006) The effect of topographical and atmospheric masses on spaceborne gravimetric and gradiometric data, Studia Geophysica et Geodaetica. 50:549-582, doi: 10.1007/s11200-006-0035-7

Petrovkaya M.S. and Vershkov A.N. (2006) Non-singular expressions for the gravity gradients in the local north-oriented and orbital reference frames, Journal of Geodesy, 80:117-127, doi: 10.1007/s00190-006-0031-2

Reference Atmosphere Committee (1961). Report of the preparatory group for an international reference atmosphere accepted at the COSPAR Meeting in Florance, April 1961. North Holland Publ. Co., Amsterdam.

Seitz K. and Heck B. (2003) Efficient calculation of topographic reductions by the use of tesseroids. Presentation at the joint assembly of the EGS, AGU and EUG, Nice, France, 6–11 April 2003.

Sjöberg L.E. (1993) Terrain effects in the atmospheric gravity and geoid correction. Bulletin Geodasique 64:178-184.

Sjöberg L.E. (1998) The atmospheric geoid and gravity corrections, Bollettino di geodesia e scienze affini-No.4, 421-435.

Sjöberg L.E. (1999) The IAG approach to the atmospheric geoid correction in Stokes's formula and a new strategy, Journal of Geodesy, 73:362-366, doi: 10.1007/s001900050254.

Sjöberg L.E. (2000) Topographic effects by the Stokes-Helmert method of geoid and quasi-geoid determinations. Journal of Geodesy, 74:255-268, doi: 10.1007/s001900050284.

Sjöberg L.E. (2001) Topographic and atmospheric corrections of gravimetric geoid determination with special emphasis on the effects of harmonics of degrees zero and one, Journal of Geodesy, 75:283-290, doi: 10.1007/s001900100174.

Sjöberg Le. E (2006) The effects of Stokes's formula for an ellipsoidal layering of the earth's atmosphere, Journal of Geodesy, 79:675-681, doi: 10.1007/s00190-005-0018-4.

Sjöberg L.E. (2007) The topographic bias by analytical continuation in physical geodesy, Journal of Geodesy, 81:345-350, doi: 10.1007/s00190-006-0112-2.

Sjöberg L.E. and Nahavandchi. H. (1999) On the indirect effect in the Stokes-Helmert method of geoid determination. Journal of Geodesy, 73:87-93, doi: 10.1007/s001900050222.

Sjöberg L.E. and Nahavandchi H. (2000) The atmospheric geoid effects in Stokes formula, Geophysical Journal International, 140:95-100, doi:10.1046/j.1365-246x.2000.00995.x.

Sjöberg L. E. (2006) The effects of Stokes's formula for an ellipsoidal layering of the Earth's atmosphere, Journal of Geodesy, 79:675-681: doi 10,1007/s00190-005-0018-4.

Sun W. and Sjöberg L.E. (2001) Convergence and optimal truncation of binomial expansions used in isostatic compensations and terrain corrections, Journal of Geodesy, 74:627-636, doi: 10.1007/s001900000125.

Tenzer R., Novák P., Moore P. and Vajda P. (2006) Atmospheric effects in the derivation of geoid-generated gravity anomalies, Studia Geophysica et Geodaetica, 50:583-593, doi: 10.1007/s11200-006-0036-6.

Tsoulis D. (2001) Terrain correction computations for a densely sampled DTM in the Bavarian Alps. Journal of Geodesy, 75:291-307, doi : 10.1007/s001900100176.

United State Standard Atmosphere (1976) Joint model of the National Oceanic and Atmospheric administration, national aeronautics and space administration and United states air force, Washington, D.C.

Wallace JM. and Hobbs PV. (1977) Atmospheric Science- An Introductory Survey, Academic press, New York

Wild F. and Heck B. (2004a) A comparison of different isostatic models applied to satellite gravity gradiometry, Gravity, Geoid and Space Missions GGSM 2004 IAG International Symposium Porto, Portugal August 30 – September 3, 2004.

Wild, F. and Heck, B. (2004b) Effects of topographic and isostatic masses in satellite gravity gradiometry. Proc. Second International GOCE User Workshop GOCE. The Geoid and Oceanography, ESA-ESRIN, Frascati/Italy, March 8-10, 2004 (ESA SP – 569, June 2004), CD-ROM.

Xu P. (1992) Determination of surface gravity anomalies using gradiometric observables, Geophysical Journal International, 110, pp. 321-332, doi:10.1111/j.1365-246X.1992.tb00877.x.

Xu P. (1998) Truncated SVD methods for discrete linear ill-posed problems, Geophysical Journal International, 135: 505-514, doi:10.1046/j.1365-246X.1998.00652.x.

Xu P. and Rummel R. (1994) A simulation study of smoothness methods in recovery of regional gravity fields, Geophysical Journal International, 117:472-486, doi:10.1111/j.1365-246X.1994.tb03945.x.

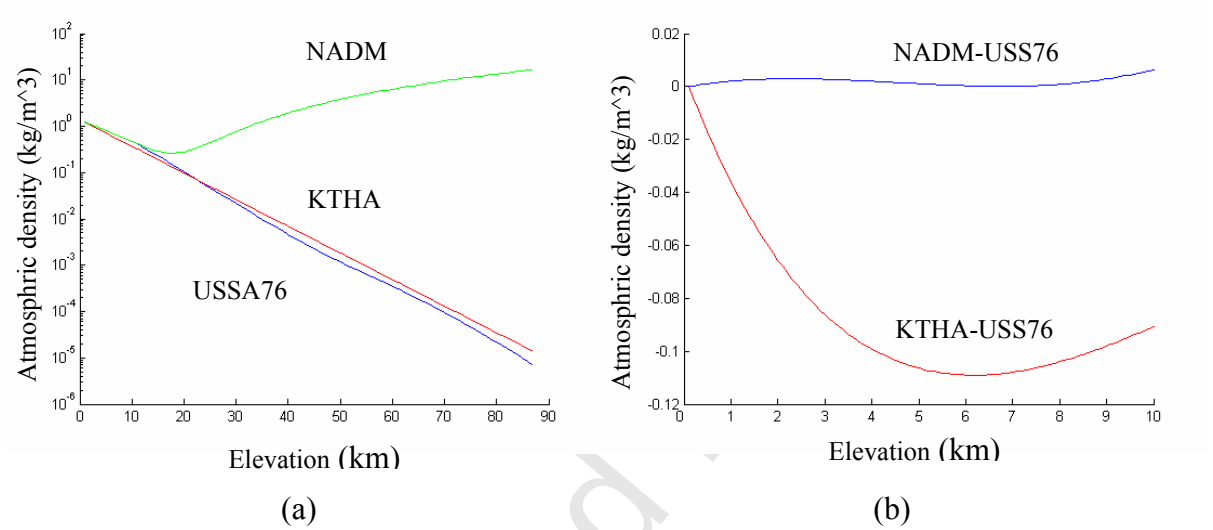

Figure 1. (a) NADM in green, KTHA in red and USSA76 in blue versus elevation (vertical axis is in logarithmic scale), (b) deference between NADM and USSA76 in blue, KTHA and USSA76 in red, respectively to 10-km elevation

Table 1. DAE on the SGG data at 250km level based on the NADM and the KTHA up to 10 km. Unit: 1mE

	NADM				KTHA			
	max	mean	min	std	max	mean	min	std
V_{uu}	-2.0069	-2.2153	-2.391	± 0.0762	-0.6957	-0.8831	-1.0405	± 0.0693
V_{vv}	-1.9238	-2.2247	-2.4123	± 0.1062	-0.6159	-0.8831	-1.0491	± 0.0966
V_{ww}	4.6257	4.4400	3.9364	± 0.1520	1.9352	1.7662	1.3171	± 0.1392
V_{uv}	0.0729	-0.0276	-0.1119	± 0.0403	0.0679	-0.0229	-0.1004	± 0.0370
V_{uw}	0.2976	0.0110	-0.2984	± 0.1125	0.2632	0.0063	-0.2706	± 0.1038
V_{vw}	0.3544	0.0125	-0.2043	± 0.0879	0.3213	0.0140	-0.1822	± 0.0809

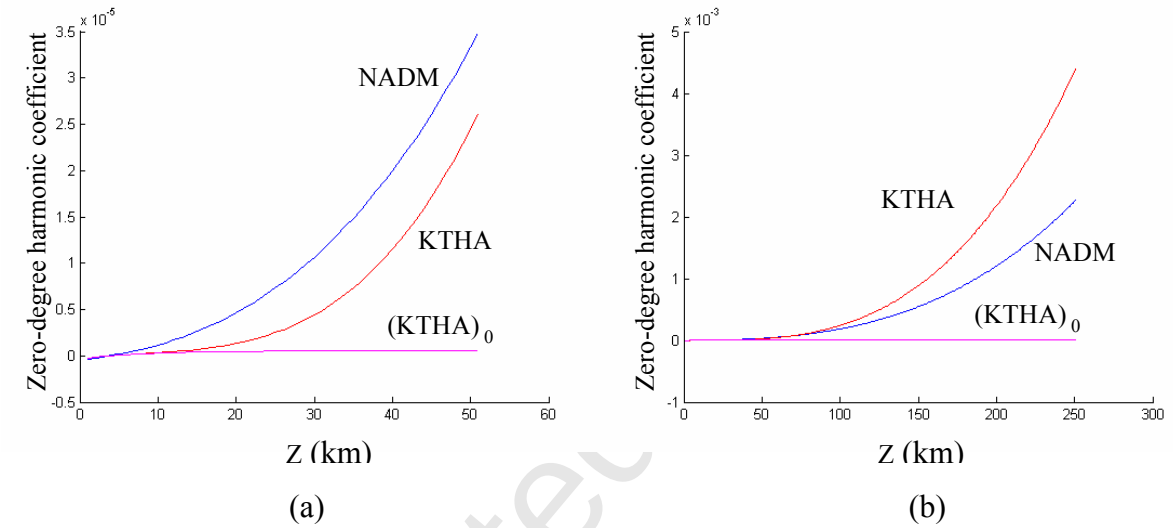

Figure 2. Behaviour of the unitless zero-degree harmonic of the atmospheric potential versus various Z. (a) Z=0 to 50 km and (b) Z=0 to 250 km

Table 2. Values of the atmospheric mass density based on the USSA61 and USSA76, Unit: kg/ m^3

Elevation (km)	USSA61	USSA76	difference
0	1.2225	1.2227	0.0002
2	1.0067	1.0047	-0.0020
4	8.2362×10^{-1}	8.1780×10^{-1}	-0.0582×10^{-1}
6	6.6511×10^{-1}	6.5888×10^{-1}	-0.0623×10^{-1}
8	5.2702×10^{-1}	5.2479×10^{-1}	-0.0223×10^{-1}
10	4.0937×10^{-1}	4.1273×10^{-1}	0.0336×10^{-1}
12	3.1131×10^{-1}	3.1135×10^{-1}	0.0004×10^{-1}
14	2.3211×10^{-1}	2.2742×10^{-1}	-0.0469×10^{-1}
16	1.7007×10^{-1}	1.6615×10^{-1}	-0.0392×10^{-1}
18	1.2289×10^{-1}	1.2142×10^{-1}	-0.0147×10^{-1}
20	8.8025×10^{-2}	8.8741×10^{-2}	0.0716×10^{-2}
30	1.8410×10^{-2}	1.8375×10^{-2}	-0.0035×10^{-2}
40	3.9957×10^{-3}	3.9878×10^{-3}	-0.0079×10^{-3}
50	1.0269×10^{-3}	1.0248×10^{-3}	-0.0021×10^{-3}

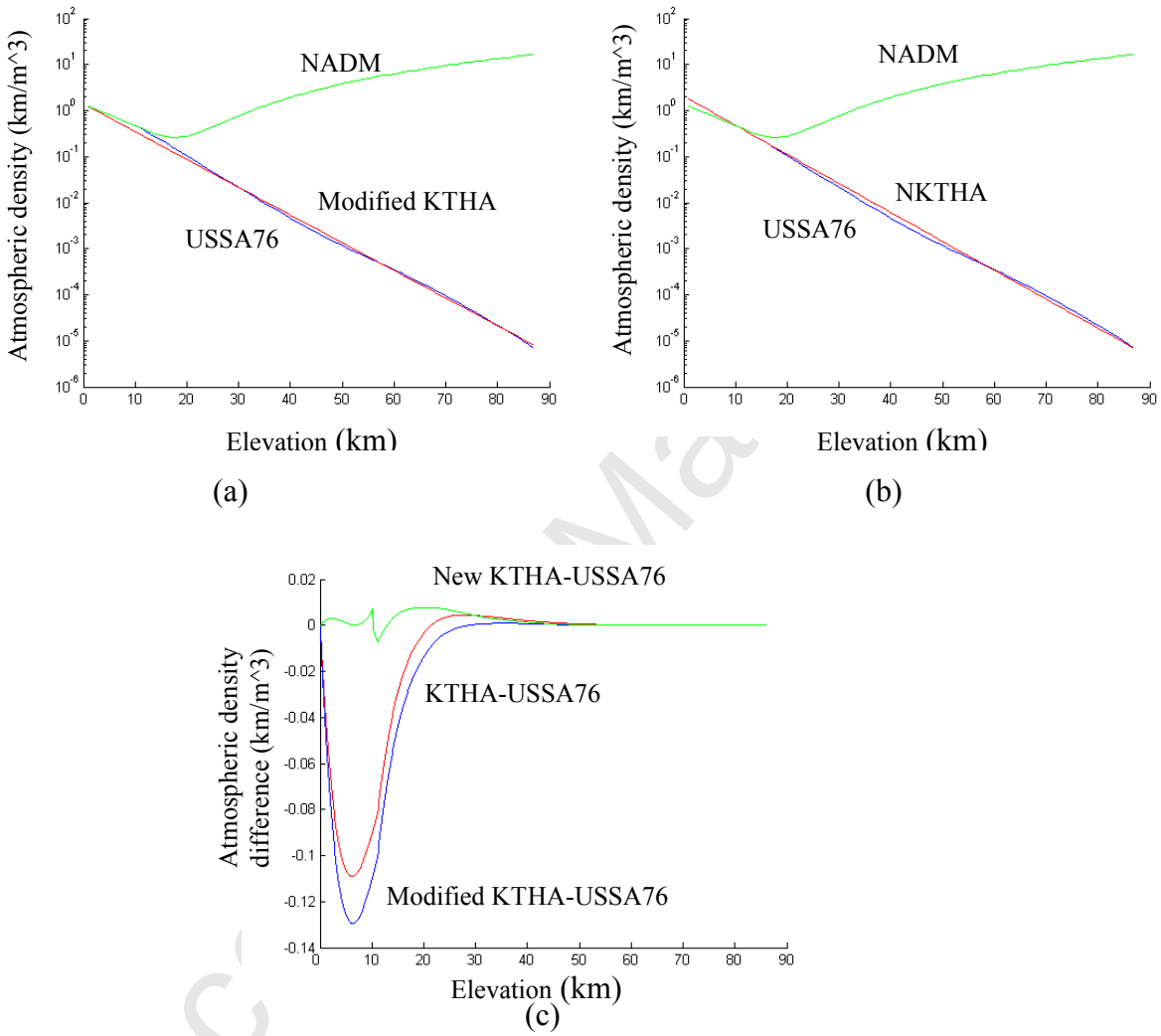

Figure 3. (a) Modified KTHA in red (vertical axis is in logarithmic scale), (b) NKTHA based on the USSA76 in red (vertical axis is in logarithmic scale), (c) differences between approximating models of KTHA, modified KTHA New KTHA and USSA76

Table 3. Statistics of DAE on the SGG data at 250 km level based on the KTHA and the modified KTHA, Unit: mE

	KTHA				Modified KTHA			
	max	mean	min	std	max	mean	min	std
V_{uu}	-0.8718	-1.0590	-1.2166	± 0.0693	-0.7800	-0.9661	-1.1228	± 0.0690
V_{vv}	-0.7920	-1.0590	-1.2249	± 0.0966	-0.7005	-0.9657	-1.1306	± 0.0961
V_{ww}	2.2875	2.1180	1.6694	± 0.1392	2.1005	1.9319	1.4859	± 0.1385
V_{uv}	0.0680	-0.0229	-0.1004	± 0.0370	0.0677	-0.0227	-0.0998	± 0.0369
V_{uw}	0.2632	0.0063	-0.2706	± 0.1038	0.2615	0.0061	-0.2691	± 0.1033
V_{vw}	0.3213	0.0140	-0.1822	± 0.0809	0.3196	0.0141	-0.1811	± 0.0805

Table 4. Statistics of the DAE on the SGG data at 250 level based on the NKTHA, Unit: mE

	NKTHA			
	max	mean	min	std
V_{uu}	-2.3564	-2.5643	-2.7406	± 0.0762
V_{vv}	-2.2733	-2.5738	-2.7617	± 0.1062
V_{ww}	5.3250	5.1381	4.6355	± 0.1520
V_{uv}	0.0729	-0.0276	-0.1119	± 0.0403
V_{uw}	0.2976	0.0110	-0.2984	± 0.1125
V_{vw}	0.3544	0.0125	-0.2043	± 0.0879

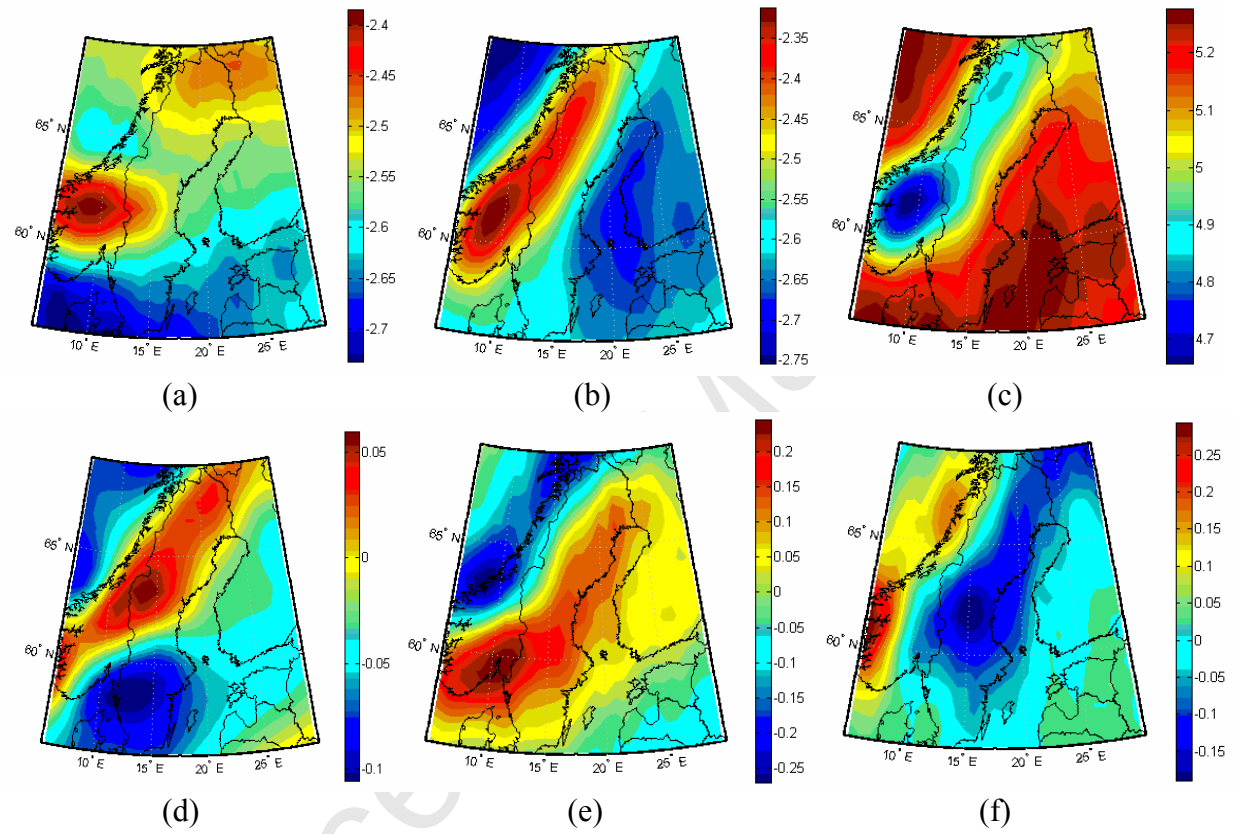

Figure 4. DAE on the SGG at 250km based on the NKTHA, (a), (b), (c), (d), (e) and (f) are V_{uu}, V_{vv}, V_{ww}, V_{uv}, V_{uw} and V_{vw}, respectively. Unit: mE